Published in final edited form as:
J Comp Neurol. 2011 August 15; 519(12): 2493–2507. doi:10.1002/cne.22637.

Sensory Neuroanatomy of *Parastrongyloides trichosuri*, a Nematode Parasite of Mammals: Amphidial Neurons of the First-Stage Larva

He Zhu[1], **Jian Li**[2], **Thomas J. Nolan**[1], **Gerhard A. Schad**[1,*], and **James B. Lok**[1,**]

[1] Department of Pathobiology, School of Veterinary Medicine, University of Pennsylvania, Philadelphia, Pennsylvania 19104

[2] Department of Neurology, School of Medicine, University of Pennsylvania, Philadelphia, Pennsylvania 19104

Abstract

Owing to its ability to switch between free-living and parasitic modes of development, *Parastrongyloides trichosuri* represents a valuable model with which to study the evolution of parasitism among the nematodes, especially aspects pertaining to morphogenesis of infective third-stage larvae. In the free-living nematode *Caenorhabditis elegans*, developmental fates of third-stage larvae are determined in part by environmental cues received by chemosensory neurons in the amphidial sensillae. As a basis for comparative study, we have described the neuroanatomy of the amphidial sensillae of *P. trichosuri*. Using computational methods we incorporated serial electron micrographs into a three-dimensional reconstruction of the amphidial neurons of this parasite. Each amphid is innervated by 13 neurons, and the dendritic processes of 10 of these extend nearly to the amphidial pore. Dendritic processes of two specialized neurons leave the amphidial channel and terminate within invaginations of the sheath cell. One of these is similar to the finger cell of *C. elegans*, terminating in digitiform projections. The other projects a single cilium into the sheath cell. The dendritic process of a third specialized neuron terminates within the tight junction of the amphid. Each amphidial neuron was traced from the tip of its dendrite(s) to its cell body in the lateral ganglion. Positions of these cell bodies approximate those of morphologically similar amphidial neurons in *Caenorhabditis elegans*, so the standard nomenclature for amphidial neurons in *C. elegans* was adopted. A map of cell bodies within the lateral ganglion of *P. trichosuri* was prepared to facilitate functional study of these neurons.

Keywords

3D reconstruction; amphidial neurons; *Caenorhabditis elegans*; *Parastrongyloides trichosuri*; *Strongyloides stercoralis*

INTRODUCTION

Amphids are paired anterior sensillae of nematodes, which play crucial roles in sensing physico-chemical cues from the environment (Bargmann et al., 1990; Bargmann and Horvitz, 1991a; Ren et al., 1996; Schackwitz et al., 1996; Pierce et al., 2001; Li et al., 2003). The anatomy of the amphids and functions of the amphidial neurons in the free-living

**Correspondence to: James B. Lok, 3800 Spruce St, PA, 19104. jlok@vet.upenn.edu, Telephone: +1-215-898-7892, Fax: +1-215-573-7023.
*Deceased

nematode *Caenorhabditis elegans* have been described in detail (Bargmann,; Ward et al., 1975; Bargmann and Horvitz, 1991b; Bargmann et al., 1993; Mori and Ohshima, 1995; Troemel et al., 1997; Pierce-Shimomura et al., 2001). Selection of a suitable model with which to adapt these methods to study the sensory neurobiology of parasitic nematodes is an important priority. Considering previous research into the functions of amphidial neurons in *C. elegans*, the essential requirements for a model parasitic nematode in which to study the structure and function of amphidial neurons would be similar morphology of the first-stage larva (L1) and a cuticle with sufficient optical transparency to allow visual observation of neurons by light microscopy and, when technology allows, detection of fluorescent reporters encoded in neuronally expressed transgenes. *Strongyloides stercoralis*, a member of the family *Strongyloididae*, was previously selected as a model based on fulfillment of these minimal criteria, and significant findings on the functions of its amphidial neurons were obtained (Ashton et al., 1998; Forbes et al., 2004; Nolan et al., 2004; Ashton et al., 2007). Although it is well suited for microlaser surgical study of neuronal function in individual specimens, the fact that *S. stercoralis* can complete only one generation of free-living development will significantly curtail application of new genetically based methods of neuronal ablation now being pioneered in *C. elegans* (Chelur and Chalfie, 2007). For this reason we are seeking an alternative model parasitic nematode more amenable to genetic manipulation for studies of sensory neurobiology.

Parastrongyloides trichosuri, a parasite of the Australian brush-tailed possum and another member of the family *Strongyloididae*, shares the aforementioned advantages of *S. stercoralis* and has the added advantage of being able to cycle indefinitely as a free-living organism that can be cultured in the laboratory on bacterial lawns using techniques similar to those that are standard for *C. elegans*. These attributes make *P. trichosuri* amenable to genetic analysis (Grant et al., 2006b), a characterization that is substantiated by the development of a robust system for transgenesis in this nematode (Grant et al., 2006a). Moreover, infective third-stage larvae (L3i) of *P. trichosuri* arise from free-living populations under conditions of crowding or depleted food resources as do the dauer larvae of *C. elegans*. These L3i are capable of infecting their marsupial host by skin penetration followed by a canonical program of parasitic development reminiscent of other members of the family *Strongyloididae*. Additionally, we have identified the sugar glider, *Petaurus breviceps*, as a small marsupial host, which can be obtained commercially and maintained in the laboratory (Nolan et al., 2007). In view of these advantages, we consider *P. trichosuri* to be a potential model for studies of sensory neurobiology that incorporate new molecular genetic approaches. This worm is particularly well suited to basic studies of specific adaptations to parasitism among the Nematoda.

In this study, we present a reconstruction based on transmission electron micrographs of serial sections of amphidial neurons of the L1 stage larvae of *P. trichosuri*. Such a reconstruction is a prerequisite for functional study of these neurons based on ablation of their cell bodies by microlaser surgery or genetically targeted cell killing. Our reconstruction includes 13 amphidial cells and two supporting cells, the socket cell and sheath cell. Additionally, unidentified cell bodies in the lateral ganglia were also reconstructed in order to establish a precise map of cells in this region for future studies.

MATERIALS AND METHODS

Parasites

The strain of *P. trichosuri* used in this study was originally obtained from a laboratory culture established with field-collected material from New Zealand (Grant et al., 2006b). The parasites were maintained in sugar gliders (Nolan et al., 2007) and in free-living plate cultures as described (Grant et al., 2006b). First-stage larvae (L1) were obtained within 12

hours of hatching from eggs collected from growing cultures of free-living *P. trichosuri* adults.

Fixation and embedding

P. trichosuri L1 were fixed by methods based on those used previously for *S. stercoralis* (Ashton et al., 1995). Freshly hatched worms were transferred into 0.5M M9 buffer with 0.3% 1-phenoxy-2-propanol for anesthesia. Anesthetized worms were placed in ice-cold 4% glutaraldehyde in 0.05 M cacodylate buffer, pH 6.8, for 3 hours. Worms were then collected from glutaraldehyde by centrifugation, rinsed three times in ice-cold 0.05 M cacodylate buffer, pH 6.8 and then post-fixed in 1% osmium tetroxide in 0.05 M cacodylate buffer, pH 6.8, for one hour at room temperature. After fixation, worms were dehydrated in an acetone series, and embedded in 1:1 Araldite 502: DDSA (Electron Microscopy Sciences, Inc., Hatfield, PA). Plastic monomers were evacuated twice by vacuum pump and polymerized at 60° C for 48 hours.

Sectioning and electron microscopy

Serial sections were cut on a Sorvall MT-2 ultramicrotome with a diamond knife, and ribbons of sections were collected on Formvar-covered single slotted grids. The sections were stained in 1.5% uranyl acetate in methanol for 17 minutes in the dark at room temperature and then for 10 minutes at room temperature with lead citrate by the Reynolds procedure (Reynolds, 1963). In order to minimize errors in tracing amphidial dendrites, three complete sets of serial sections extending posterior from the tip of head through the nerve ring to the lateral ganglion were prepared with two different average thicknesses: one setat 150-nm and two sets at 90-nm thickness. Serial sections were observed and images of them captured into Tiff digital image stacks using a JEOL 1010 transmission electron microscope operating at 80KV at the Biomedical Imaging Core of University of Pennsylvania.

Tracing and three-dimensional reconstruction

Three-dimensional reconstructions of the sensory neuroanatomy were made by importing Tiff digital image stacks into the Imod© (Boulder Laboratory for 3-Dimensional Electron Microscopy of Cells and the Regents of the University of Colorado) software package for tracing, contour-based volume segmentation and meshing (Kremer et al., 1996). Sensory neuroanatomic structures of the right amphid were traced manually, section by section, in order to account for the extremely small changes that can occur between adjacent sections and thereby generate an accurate three dimensional reconstruction. Structures of the left amphid were traced in every tenth section to confirm symmetry between the two amphids.

Neuronal dye filling studies

Patterns of fluorescent dye uptake into amphidial neurons were observed in newly hatched first-stage larvae of *P. trichosuri*. We employed two dyes, which have been used previously for neuronal dye filling studies in other nematodes: 5-fluorescein isothiocyanate (FITC) and DiI. Studies with FITC were conducted as described (Hedgecock et al., 1985). Stock solutions containing 20 mg/ml of FITC in dimethylformamide were prepared and stored −20° C until use. For dye filling experiments FITC stock was diluted 1:50 in M9 buffer to give a working solution of 0.4 mg/ml. Studies with DiI were carried out as described (Shaham, 2006). Stock solutions containing 2 mg/ml of DiI were prepared in dimethylformamide and stored at −20° C until use. For dye filling experiments a working solution containing 0.02 mg/ml of DiI was prepared by diluting the dimethylformamide stock solution 1:100 in M9 buffer. For both FITC and DiI, *P. trichosuri* larvae were incubated for two hours at room temperature in the working solution of dye, washed three

times in M9 buffer and then incubated for two hours on NGM agar plates with *E. coli* HB101 lawns to allow clearance of ingested dye from their digestive tracts. Dye treated worms were mounted on 3% agar pads containing 1-phenoxy-2-propanol as an anesthetic and examined by differential interference constrast (DIC) and fluorescence microscopy. Images were captured with a Spot RT Color digital camera and processed using either the Spot Advanced image analysis software package (Diagnostic Instruments, Inc., Sterling Heights, Michigan, USA) or Adobe Photoshop 7.0. All image processing algorithms (eg. brightness and contrast adjustments) were applied in a linear fashion to the entire image.

Nomenclature

The amphidial neurons of *P. trichosuri* were named using the nomenclature for amphidial neurons of *C. elegans* (White et al., 1986). In this schema, three letters are used per name: the first letter is A for amphid; the second letter is either S (single) for the neurons that have one dendritic process or D (double) for those with two such processes. The specialized wing cells of *C. elegans* are identified by a W and the finger cells by F in the second position. In *C. elegans*, there are 12 neurons in the amphidial complex, and each neuron is assigned a third letter, from A to L (Ward et al., 1975). In assigning three-letter designations to the neurons of *P. trichosuri*, first letters were always A, and second letters were based on morphologies of dendrites of individual neurons. The third letters were assigned based on comparison of positions of neuronal cell bodies in the lateral ganglia of *P. trichosuri* to those of *C. elegans*.

RESULTS

Visual interpretation of serial sections

All visual interpretations and three-dimensional reconstructions were based on complete sets of serial sections from three first-stage *P. trichosuri* larvae, one at 150 nm thickness and two at 90 nm thickness. There was virtually complete consistency between morphological features seen in comparable sections from these three sets.

There are 13 pairs of amphidial neurons in *P. trichosuri*, with one member of each pair per amphid. Each bipolar amphidial neuron consists of a dendritic process in the form of a modified cilium, a dendrite, a cell body, and an axon. Each amphidial channel is formed by a socket cell and a sheath cell and contains 11 amphidial cilia, which contact the external environment via the amphidial pore. The opening of the amphidial channel, lying approximately 2 μm from the cephalic extremity, is formed by the socket cell, which parallels the amphidial channel and takes on dendrite-like morphology beginning with the 42nd section, approximately 4.5 μm posterior to the amphidial opening (Fig. 1A, C). At this same level, the sheath cell connects with the socket cell by a tight junction and encloses the left cavity of the amphidial channel without forming a self-tight junction. The longest cilium in the amphidial channel extends to within approximately 1.5 μm of the amphidial opening, and the other cilia terminate at different levels within the amphidal channel (Fig. 1B). Approximately 5μm posterior to the amphidial pore, the two digitiform dendrites of the finger cell AFD and the single dendrite of ASC extend ventrally and laterally from the amphidial channel into pockets within the sheath cell. Thus, the dendrites of these two cells do not communicate directly with the external environment (Fig. 1D). In the transition zone, where cilia with doublet microtubules and single microtubules transform to dendrites with only singlet microtubules, the two projections of the finger cell merge into one dendrite in which only singlet microtubules can be found. All other dendrites have both singlet and doublet microtubules (Fig. 1E). Approximately 9.5 μm from the amphidial pores, the dendrites enlarge and become irregular in shape (Fig. 1E). In the next four or five sections (comprising a zone 0.4 μm wide), all of the amphidial neuronal processes form tight

junctions with each other and with the sheath cell (Fig. 1F). As with *Strongyloides stercoralis* and *Haemonchus contortus*, tight junctions of all amphidial neurons in *P. trichosuri* appear at the same level, while those in *C. elegans* occur at different levels (Ward et al., 1975; Ashton et al., 1995; Ashton et al., 1999). The single dendritic process of ASM, the shortest dendrite of those observed in *P. trichosuri* terminates at the level of the tight junction (Fig. 1F). This morphology is similar to that of ASA in *S. stercoralis*. Posterior to the tight junction region, the sheath cell, like the socket cell, changes to a dendrite-like process, which continues in a loose bundle with the socket cell and the dendritic processes of all 13 amphidal neurons posterior toward the nerve ring (Fig. 2). The individual dendrites in the bundle are irregular in shape and vary in thickness. For this reason, a set of 60 nm-thick serial sections was prepared from the region just posterior of the amphidial tight junction to minimize differences between adjacent sections and thereby enhance the accuracy of tracing the neuronal processes. Beginning approximately 33 μm from the amphidial pore, the dendrite-like process of the socket cell enlarges and merges into its cell body (Fig. 3). The anterior margin of the nerve ring appears approximately 57 μm from the amphidial pore and runs through the next 40 sections (2.4 μm). The dendritic bundles bypass the nerve ring near its lateral surface (Fig. 4). The cell bodies in the lateral ganglia, including those of the amphidial neurons, appear just posterior to the nerve ring. The cell bodies of AFD-class neurons are the most anterior of the amphidial neurons, being positioned approximately 61μm from the amphidial pores (Fig 5). The other individual dendrites, including those of the sheath cells, exit the bundles and connect to their corresponding cell bodies at different levels within the lateral ganglia.

Three-dimensional reconstructions

Three-dimensional reconstructions were made to better understand the structure of the amphids and positional relationships of neurons within them. The reconstructions show the neuronal processes with the socket and sheath cells from their anterior-most tips through the lateral ganglia (Fig. 6A). The three-dimensional model of the anterior amphids (Fig. 6B, C) indicates the presence of a socket cell, a sheath cell, a finger cell and twelve single cilium cells in each amphid. The uniciliate sensory neurons, designated ASA, ASB, ASC, ASE, ASF, ASG, ASH, ASI, ASJ, ASK, ASM, terminate near the amphidial pore and have similar simple morphology within the amphidial channels. The finger cell, AFD, projects seven to eight finger-like sensory cilia into pockets within the sheath cell where they terminate. Unlike other uniciliate dendrites, ASC projects its cilium into a pocket within the sheath cell.

Figure 7A is a model of cell bodies in the right lateral ganglion. This reconstruction comprises not only the 13 amphidial neurons, which were traced from the tips of their dendritic processes to their cell bodies, but also unidentified cell bodies in the right lateral ganglion as well. Thus, the spatial relationships between all cell bodies in the lateral ganglia may be discerned. This feature will facilitate identification of individual neurons for functional study by microlaser surgery or genetically targeted cell killing.

Arrangement of dendritic processes at the tight junction

One criterion used in comparative study of amphidial neuronal anatomy in various species of nematode is the arrangement of dendritic processes within the amphidial bundle viewed in cross section (Ward et al., 1975; Ashton et al., 1995; Li et al., 2000; Li et al., 2001; Bumbarger et al., 2009). We compared this arrangement in cross sections taken at the level of the tight junction of *P. trichosuri* L1 (diagrammed in Fig. 8) to similar data from the parasitic nematode *Haemonchus contortus* (Li et al., 2000) and the microbe-feeding nematode *Acrobeles complexus* (Bumbarger et al., 2009). The arrangement of dendrites in *P. trichosuri* was generally more similar to that in *H. contortus* than to that in *A. complexus*.

Marked similarities in dendritic position were seen in six neurons (ASA, ASB/ADB, AFD, ASE, ASG and ASJ) of *P. trichosuri* and *H. contortus* (Fig. 8). If, as we consider likely, the unidentified dendrite in the amphidial bundle of *H. contortus* is that of ASM, then the number of dendrites with similar positions to those in *P. trichosuri* increases to seven. By contrast, positions of only two dendrites (those of ASE and ASJ) were similar in *P. trichosuri* and *A. complexus* (Fig. 8).

Neuronal dye filling studies

No amphidial neurons in *P. trichosuri* L1 took up FITC. However, the amphidial channels of these larvae filled with this dye (Fig. 9A, B). A single pair of amphidial neurons took up DiI. These neurons have a single dendritic process extending to the amphidial pore and an axon extending to the nerve ring (Fig. 10B). The cell bodies of neurons staining with DiI in *P. trichosuri* L1 are located just anterior to the pharyngeal bulb and are the most dorsal of the amphidial cell bodies in this region (Fig. 10A, B). After comparing this position to the 3-dimensional reconstruction of the lateral ganglia of *P. trichosuri* L1 (Fig. 7), we tentatively identify the DiI-staining pair of neurons as ASL.

DISCUSSION

Since they are well characterized both anatomically (Ward et al., 1975; Ware et al., 1975) and functionally (Bargmann et al., 1993), we used the amphidial neurons of *C. elegans* as a basis for the comparative anatomical study of *P. trichosuri*. Each amphid in *C. elegans* contains 12 sensory neurons. These include three specialized neurons with flattened dendritic processes known as wing cells, a finger cell featuring a large number of microvillar projections, two neurons with double ciliate processes and six neurons with single ciliate process (Ward et al., 1975). The wing cells, which detect volatile substances (Bargmann et al., 1993) and the finger cell, which has thermosensory function (Mori and Ohshima, 1995), terminate within pockets or invaginations of the sheath cell membrane, and so do not communicate with environment directly. Dendrites of the other eight neurons extend through the amphidial channels and communicate with the environment directly through the amphidial pores.

The structures of the amphidial neurons of *P. trichosuri* are similar to those of *C. elegans* but there are differences that may indicate some important, as yet unknown, adaptations for host-finding or other function related to parasitism. These differences may also reflect the phylogenetic divergence of the genera *Caenorhabditis* and *Parastrongyloides*, which belong to Clades IV and V, respectively, in the contemporary molecular phylogeny of nematodes (Blaxter et al., 1998). Each amphid of *P. trichosuri* has a neuron, designated AFD, with complex dendritic processes sharing some morphologic characteristics with the finger cell (AFD) of *C. elegans.* In *C. elegans*, the finger cell dendrite, which contains singlet microtubules, has myriad tiny microvillus-like projections terminating dorsal to the amphidial channel in a pocket within the sheath cell. By contrast, dendritic processes of AFD in *P. trichosuri* have only seven to eight larger finger-like projections terminating in a pocket of the sheath cell ventral to the amphidial channel. Like the dendritic processes of AFD in *C. elegans*, those of *P. trichosuri* have singlet microtubules only. The cell bodies of AFD-class neurons in *P. trichosuri*, like those of the finger cells in *C. elegans*, are the most anterior of the amphidial cell bodies in the lateral ganglia (Fig. 5). For these reasons, we hypothesize that AFD-class neurons of *P. trichosuri* are homologs of the finger cells (AFD) in *C. elegans* and have similar thermosensory functions.

In *C. elegans*, the wing cells are unusually shaped neurons that do not traverse the entire amphidial channel but rather terminate within invaginations of the sheath cell. The microtubules of the dendrites within the amphidial channels and of the three wing cells

change from singlet to doublet within the transition zone, whereas no doublet microtubules appear in the finger cells (Ward et al., 1975). Similarly, dendrites in the amphidial channels of *P. trichosuri* and those of ASChave both singlet and doublet microtubules. By contrast, AFD, which terminates within the sheath cell of *P. trichosuri*, has only singlet microtubules. Based upon these morphological similarities, we hypothesize that ASC neurons in *P. trichosuri* are the homologs of one of three pairs of wing cells in *C. elegans*. Under this hypothesis, ASC neurons of *P. trichosuri* would serve to detect volatile chemical cues (Bargmann et al., 1993), a potentially crucial function in host finding by infective larvae of this skin-penetrating parasite.

The anterior neuroanatomy of *P. trichosuri* is extraordinarily similar to that of *S. stercoralis*, another member of the family Strongyloididae. Both *P. trichosuri* and *S. stercoralis* have 13 amphidial neurons, 12 with single ciliae and one with complex dendritic processes. They are also similar in that their shortest amphidial neurons (ASM) terminate at the bases of their amphidial channels. *P. trichosuri* and *S. stercoralis* both have specialized neurons, the finger cell AFD and lamellar cell ALD, respectively, which bear complex dendritic processes terminating within invaginations ofthe sheath cell. The dendritic processes of the finger cell of *P. trichosuri* and the lamellar cell of *S. stercoralis* both terminate ventral to the amphidial channels.

The cell bodies of amphidial neurons of *S. stercoralis* are positioned in the lateral ganglia similarly to those of *C. elegans*. With the exception of ASA, ASB and ASC, which are located anterior of nerve ring, all other amphidial neurons located in lateral ganglia of *S. stercoralis* were named by the positional comparison to amphidial neurons of *C. elegans* (Ashton et al., 1998; Ashton et al., 1999). This process allows positional homologs to be tentatively identified and functions to be hypothesized. In *P. trichosuri*, the cell bodies of amphidial neurons are also in positions similar to those in *S. stercoralis* and *C. elegans. P. trichosuri* differs from *S. stercoralis* and resembles *C. elegans* in that cell bodies of all 13 amphidial neurons are located posterior to the nerve ring.

Comparative anatomical studies of anterior sensory neurons in nematodes have been based positions of amphidial cell bodies in the lateral ganglion and the morphology of dendritic processes and the location of their termini either near the amphidial pore or within invaginations of the sheath cell. In addition, the arrangement of dendrites in the amphidial bundle has also served as a criterion (Ward et al., 1975; Ashton et al., 1995; Li et al., 2000; Li et al., 2001; Bumbarger et al., 2009). Our comparison of the arrangement of dendrites in *P. trichosuri* L1 to the same character in *H. contortus* and *A. complexus* revealed a closer concordance between *P. trichosuri* and *H. contortus* than between *P. trichosuri* and *A. complexus*. This result is inconsistent with the contemporary concept of the phylogenetic relationships of these worms (Blaxter et al., 1998) in which *P. trichosuri* and *A. complexus* inhabit Clade IV and *H. contortus* represents Clade V. The possibility that this result reflects real differences in sensory neuronal anatomy cannot be discounted, especially in view of the respective parasitic and microbiverous life histories of *P. trichosuri* and *A. complexus*. However, it is also possible that this inconsistency is due to different approaches to tentatively identifying amphidial neurons in the species under study. Our approach in the present study of *P. trichosuri*, and that of Li et al (2001) in their study of *H. contortus* both involved tracing the dendritic processes of each amphidial neuron from its origin in the amphidial channel to its cell body in the lateral ganglion. The amphidial neurons of *P. trichosuri* and *H. contortus* were then tentatively identified based on the positions of their cell bodies relative to similarly positioned amphidial neuronal cell bodies in *C. elegans* (Ward et al., 1975). By contrast tentative identifications of neurons in *A. complexus* (Bumbarger et al., 2009) were based largely on comparison of the arrangement of its amphidial dendrites at the posterior entrance to the sheath cell to the same character in third-

stage *S. stercoralis* larvae (Ashton et al., 1995). This ambiguity underscores the highly tentative nature of neuronal identities based solely on positional homology with a standard organism (eg. *C. elegans*) and also the need for caution in making comparisons between neurons tentatively identified based on different criteria.

The present finding that no amphidial neurons in *P. trichosuri* L1 fill with FITC constrasts starkly with the FITC filling pattern in *C. elegans* in which amphidial neuron pairs ASH, ASI, ASJ, ASK ADF and ADL take up this dye (Hedgecock et al., 1985). Similarly, whereas six pairs of amphidial neurons in *C. elegans* (ASH, ASI, ASJ, ASK ADL and AWB) take up DiI, only a single neuron pair in *P. trichosuri* L1, tentatively identified as ASL, does so. This result represents a departure from a conserved pattern of dye filling in amphidial neurons seen in a wide range of free-living and insect-associated nematodes spanning phylogenetic Clades IV and V (Blaxter et al., 1998; Srinivasan et al., 2008) and may reflect as yet unknown adaptations in neuronal physiology or structure that are specific to animal parasitism. Nevertheless, it is noteworthy that the single amphidial neuron in *P. trichosuri* that takes up DiI (ASL) is the positional homolog of one that does so in *C. elegans* (ADL). This observation, alongside cell body position and dendritic morphology, constitutes a third line of evidence supporting our identification of this neuron in *P. trichosuri* as ASL. From a practical standpoint, future functional studies of individual neurons in *P. trichosuri*, either by microlaser ablation or genetically targeted cell killing, will require examination of neuronal cell bodies by light microscopy. Therefore, the map of amphidial cell bodies (Fig 7B) that we have prepared based on our 3-dimensional reconstruction of the lateral ganglion (Fig. 7A) will have to be reconciled with views of this structure that can be obtained by DIC microscopy. Tentative identification of the cell bodies of ASL neurons by position and DiI filling provides a useful landmark with which to begin this process.

Following from these lines of evidence, we have proposed a hypothetical nomenclature for the amphidial neurons of *P. trichosuri* based on that of their positional homologs in *C. elegans*. The validity of this nomenclature, and the overall homologies implicit in it, remain to be tested by functional studies of the amphidial neurons of *P. trichosuri*. Such confirmatory functional studies, involving neuronal ablation by microlaser surgery and observation of resulting changes in behavior and development may eventually be augmented by additional lines of evidence based on conserved expression patterns of neuron specific genes. The feasibility of transgenesis and other molecular biological methods necessary for such studies has already been demonstrated for *P. trichosuri* (Grant et al., 2006a; Grant et al., 2006b; Newton-Howes et al., 2006).

Functional studies have generally supported the designations of amphidial neurons in *S. stercoralis* and *Ancylostoma caninum* based on positional similarity of cell bodies to *C. elegans* (Ashton et al., 1998; Lopez et al., 2000; Forbes et al., 2004; Ketschek et al., 2004; Nolan et al., 2004; Ashton et al., 2007). For example, neurons designated ASE and ASH in both *S. stercoralis* and *C. elegans* mediate chemoattaction and chemorepulsion (Bargmann and Horvitz, 1991a; Forbes et al., 2004). In similar fashion, ADL and ASH mediate avoidance of noxious chemicals in *C. elegans* and *A. caninum* (Bargmann and Horvitz, 1991a; Ketschek et al., 2004). Moreover, *C. elegans* and *S. stercoralis* appear to exert similar neuronal control over temperature-sensitive processes. In *C. elegans* thermotaxis is controlled by AFD-class neurons (Mori and Ohshima, 1995) and the positional homologs of these neurons, the ALD class, control both thermotaxis and temperature-regulated developmental switching in *S. stercoralis*. (Lopez et al., 2000; Nolan et al., 2004). Finally, just as ASI- and ADF-class neurons mediate dauer formation and ASJ-class neurons mediate dauer recovery in *C. elegans* (Bargmann and Horvitz, 1991b), the morphogenetically similar processes of L3i formation and reactivation in *S. stercoralis* depend upon ASI- and ASF-class and ASJ-class neurons, respectively (Ashton et al., 1998; Ashton et al., 2007). The

advantages that *P. trichosuri* offers as a model organism for the study of adaptations to parasitism among nematodes, chiefly the ability to cycle indefinitely as a free-living organism in laboratory culture and switch to a parasitic mode of development in response to shifts in culture environment argue strongly for a focused effort to translate contemporary functional neurobiological methodology to it from *C. elegans* and from its less tractable relative *S. stercoralis*. The anatomical reconstruction we describe here represents an important first step in that process.

Acknowledgments

Supporting Grants: This study was supported by grants R01 AI022262 (to JBL) and R01 RR02512 (to M. Haskins) from the U.S. National Institutes of Health.

We thank Prof. Warwick Grant, La Trobe University, Australia for the original starting material for our culture of *P. trichosuri*. We are grateful to Dr. Norman Wiltshire and the animal husbandry staff of the University of Pennsylvania Laboratory Animal Resources group for their excellent care of the sugar gliders used as hosts of *P. trichosuri* in this study. We are also grateful to two anonymous reviewers for helpful and constructive critiques of the manuscript.

LITERATURE CITED

Ashton FT, Bhopale VM, Fine AE, Schad GA. Sensory neuroanatomy of a skin-penetrating nematode parasite: *Strongyloides stercoralis*. I. Amphidial neurons. Journal of Comparative Neurology. 1995; 357:281–295. [PubMed: 7665730]

Ashton FT, Bhopale VM, Holt D, Smith G, Schad GA. Developmental switching in the parasitic nematode *Strongyloides stercoralis* is controlled by the ASF and ASI amphidial neurons. Journal of Parasitology. 1998; 84:691–695. [PubMed: 9714195]

Ashton FT, Li J, Schad GA. Chemo- and thermosensory neurons: structure and function in animal parasitic nematodes. Veterinary Parasitology. 1999; 84:297–316. [PubMed: 10456420]

Ashton FT, Zhu X, Boston R, Lok JB, Schad GA. *Strongyloides stercoralis*: Amphidial neuron pair ASJ triggers significant resumption of development by infective larvae under host-mimicking in vitro conditions. Experimental Parasitology. 2007; 115:92–97. [PubMed: 17067579]

Bargmann, CI. WormBook. The C. elegans Research Community. WormBook; 2006. Chemosensation in *C. elegans*. http://www.wormbook.org

Bargmann CI, Hartwieg E, Horvitz HR. Odorant-selective genes and neurons mediate olfaction in *C. elegans*. Cell. 1993; 74:515–527. [PubMed: 8348618]

Bargmann CI, Horvitz HR. Chemosensory neurons with overlapping functions direct chemotaxis to multiple chemicals in *C. elegans*. Neuron. 1991a; 7:729–742. [PubMed: 1660283]

Bargmann CI, Horvitz HR. Control of larval development by chemosensory neurons in *Caenorhabditis elegans*. Science. 1991b; 251:1243–1246. [PubMed: 2006412]

Bargmann CI, Thomas JH, Horvitz HR. Chemosensory cell function in the behavior and development of *Caenorhabditis elegans*. Cold Spring Harb Symp Quant Biol. 1990; 55:529–538. [PubMed: 2132836]

Blaxter ML, DeLey P, Garey JR, Liu LX, Scheldeman P, Vierstraete A, Vanfleteren JR, Mackey LY, Dorris M, Frisse LM, Vida JT, Thomas WK. A molecular evolutionary framework for the phylum Nematoda. Nature. 1998; 392:71–75. [PubMed: 9510248]

Bumbarger DJ, Wijeratne S, Carter C, Crum J, Ellisman MH, Baldwin JG. Three-dimensional reconstruction of the amphid sensilla in the microbial feeding nematode, *Acrobeles complexus* (Nematoda: Rhabditida). J Comp Neurol. 2009; 512:271–281. [PubMed: 19003904]

Chelur DS, Chalfie M. Targeted cell killing by reconstituted caspases. Proc Natl Acad Sci U S A. 2007; 104:2283–2288. [PubMed: 17283333]

Forbes WM, Ashton FT, Boston R, Zhu X, Schad GA. Chemoattraction and chemorepulsion of *Strongyloides stercoralis* infective larvae on a sodium chloride gradient is mediated by amphidial neuron pairs ASE and ASH, respectively. Veterinary Parasitology. 2004; 120:189–198. [PubMed: 15041094]

Grant WN, Skinner SJM, Howes JN, Grant K, Shuttle worth G, Heath DD, Shoemaker CB. Heritable transgenesis of *Parastrongyloides trichosuri*: a nematode parasite of mammals. International Journal for Parasitology. 2006a; 36:475–483. [PubMed: 16500659]

Grant WN, Stasiuk S, Newton-Howes J, Ralston M, Bisset SA, Heath DD, Shoemaker CB. *Parastrongyloides trichosuri*, a nematode parasite of mammals that is uniquely suited to genetic analysis. Int J Parasitol. 2006b; 36:453–466. [PubMed: 16500655]

Hedgecock EM, Culotti JG, Thomson JN, Perkins LA. Axonal guidance mutants of *Caenorhabditis elegans* identified by filling sensory neurons with fluorescein dyes. Dev Biol. 1985; 111:158–170. [PubMed: 3928418]

Ketschek AR, Joseph R, Boston R, Ashton FT, Schad GA. Amphidial neurons ADL and ASH initiate sodium dodecyl sulphate avoidance responses in the infective larva of the dog hookworm *Anclyostoma caninum*. Int J Parasitol. 2004; 34:1333–1336. [PubMed: 15542093]

Kremer JR, Mastronarde DN, McIntosh JR. Computer visualization of three-dimensional image data using IMOD. J Struct Biol. 1996; 116:71–76. [PubMed: 8742726]

Li J, Ashton FT, Gamble HR, Schad GA. Sensory neuroanatomy of a passively ingested nematode parasite, *Haemonchus contortus*: amphidial neurons of the first stage larva. J Comp Neurol. 2000; 417:299–314. [PubMed: 10683605]

Li J, Zhu X, Ashton FT, Gamble HR, Schad GA. Sensory neuroanatomy of a passively ingested nematode parasite, *Haemonchus contortus*: amphidial neurons of the third-stage larva. J Parasitol. 2001; 87:65–72. [PubMed: 11227904]

Li W, Kennedy SG, Ruvkun G. *daf-28* encodes a *C. elegans* insulin superfamily member that is regulated by environmental cues and acts in the DAF-2 signaling pathway. Genes Dev. 2003; 17:844–858. [PubMed: 12654727]

Lopez PM, Boston R, Ashton FT, Schad GA. The neurons of class ALD mediate thermotaxis in the parasitic nematode, *Strongyloides stercoralis*. International Journal for Parasitology. 2000; 30:1115–1121. [PubMed: 10996330]

Mori I, Ohshima Y. Neural regulation of thermotaxis in *Caenorhabditis elegans*. Nature. 1995; 376:344–348. [PubMed: 7630402]

Newton-Howes J, Heath DD, Shoemaker CB, Grant WN. Characterisation and expression of an Hsp70 gene from *Parastrongyloides trichosuri*. Int J Parasitol. 2006; 36:467–474. [PubMed: 16469320]

Nolan TJ, Brenes M, Ashton FT, Zhu X, Forbes WM, Boston R, Schad GA. The amphidial neuron pair ALD controls the temperature-sensitive choice of alternative developmental pathways in the parasitic nematode, *Strongyloides stercoralis*. Parasitology. 2004; 129:753–759. [PubMed: 15648698]

Nolan TJ, Zhu X, Ketschek A, Cole J, Grant W, Lok JB, Schad GA. The sugar glider (*Petaurus breviceps*): a laboratory host for the nematode *Parastrongyloides trichosuri*. J Parasitol. 2007; 93:1084–1089. [PubMed: 18163342]

Pierce SB, Costa M, Wisotzkey R, Devadhar S, Homburger SA, Buchman AR, Ferguson KC, Heller J, Platt DM, Pasquinelli AA, Liu LX, Doberstein SK, Ruvkun G. Regulation of DAF-2 receptor signaling by human insulin and *ins-1*, a member of the unusually large and diverse *C. elegans* insulin gene family. Genes Dev. 2001; 15:672–686. [PubMed: 11274053]

Pierce-Shimomura JT, Faumont S, Gaston MR, Pearson BJ, Lockery SR. The homeobox gene *lim-6* is required for distinct chemosensory representations in *C. elegans*. Nature. 2001; 410:694–698. [PubMed: 11287956]

Ren P, Lim CS, Johnsen R, Albert PS, Pilgrim D, Riddle DL. Control of *C. elegans* larval development by neuronal expression of a TGF-beta homolog. Science. 1996; 274:1389–1391. [PubMed: 8910282]

Reynolds ES. The use of lead citrate at high pH as an electron-opaque stain in electron microscopy. J Cell Biol. 1963; 17:208–212. [PubMed: 13986422]

Schackwitz WS, Inoue T, Thomas JH. Chemosensory neurons function in parallel to mediate a pheromone response in *C. elegans*. Neuron. 1996; 17:719–728. [PubMed: 8893028]

WormBook. WormBook: Methods in Cell Biology. In: Shaham, S., editor. C. elegans Research Community. WormBook; 2006. http://www.wormbook.org

Srinivasan J, Durak O, Sternberg PW. Evolution of a polymodal sensory response network. BMC Biol. 2008; 6:52. [PubMed: 19077305]

Troemel ER, Kimmel BE, Bargmann CI. Reprogramming chemotaxis responses: sensory neurons define olfactory preferences in *C. elegans*. Cell. 1997; 91:161–169. [PubMed: 9346234]

Ward S, Thomson N, White JG, Brenner S. Electron microscopical reconstruction of the anterior sensory anatomy of the nematode *Caenorhabditis elegans*. J Comp Neurol. 1975; 160:313–337. [PubMed: 1112927]

Ware RW, Clark D, Crossland K, Russell RL. The nerve ring of the nematode *Caenorhabditis elegans*: sensory input and motor output. Journal of Comparative Neurology. 1975; 162:71–110.

White JG, Southgate E, Thomson JN, Brenner S. The structure of the nervous system of the nematode *Caenorhabditis elegans*. Philosophical Transactions of the Royal Society of London. 1986; 314:1–340.

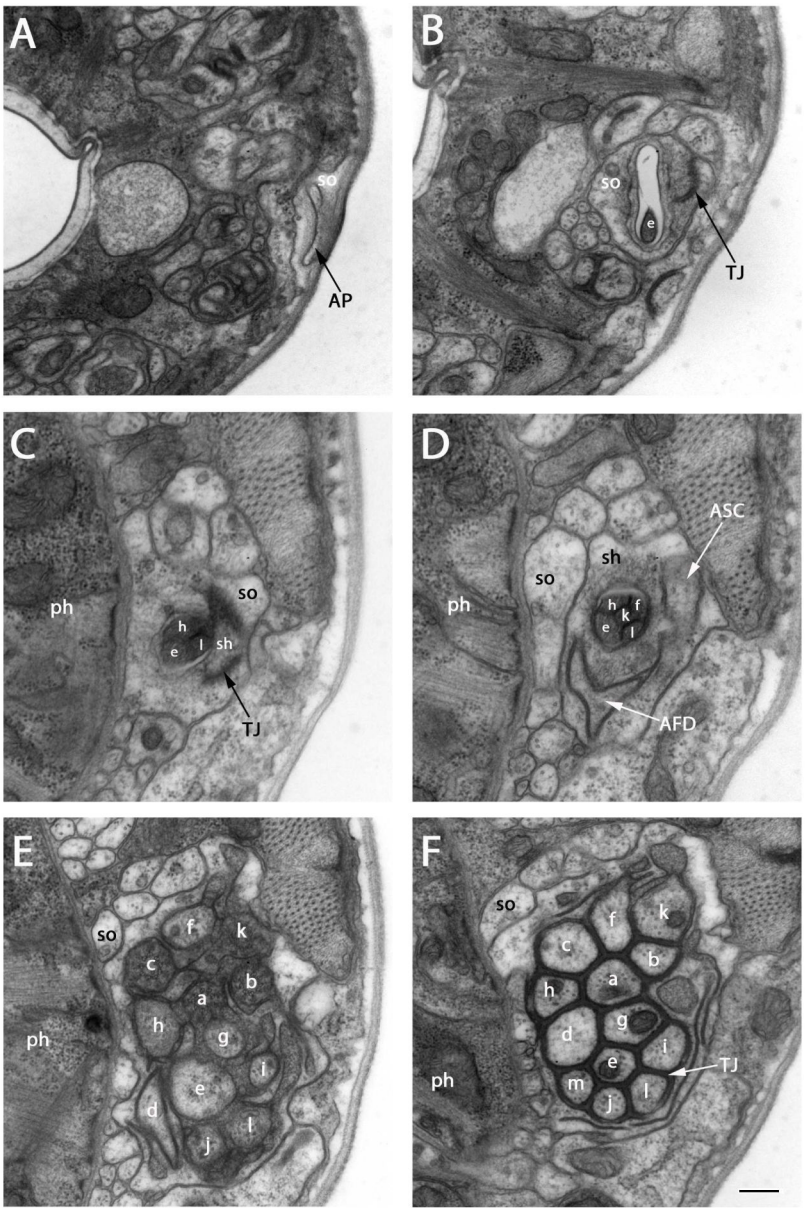

Figure 1.

Transmission electron micrographs of lateral sections at several levels between amphidial pores and the tight junction region of *P. trichosuri*. The sensory dendrites of ASA (a), ASB (b), ASC (c), AFD (d), ASE (e), ASF (f), ASG (g), ASH (h), ASI (i), ASJ (j), ASK (k), ASL (l) and ASM (m) are shown. **A:** Section approximately 2 μm posterior to the cephalic extremity. The amphidial pore (AP), which is formed by the socket cell (so) and communicates with the external environment is seen. **B:** Section approximately 1.5 μm posterior to the amphidial pore. At this level the cross section of ASE is found within the amphidial channel formed by the socket cell (so). TJ indicates the self-tight junction of the socket cell. **C:** Section approximately 4.5 μm posterior to the amphidial pore. Cross sections of three neurons, ASE, ASH and ASL, are found within the amphidial channel formed by the sheath cell (sh; ph=pharynx). This level contains the transition zone between the socket cell and the sheath cell. (TJ) (see above) indicates the tight junction between these two cells. **D:** Section approximately 5 μm posterior to the amphidial pore. Cross sections of five

neurons, ASE, ASF, ASH, ASK and ASL, are found within the amphidial channel at this level. The finger-like projection (white arrow) of the finger cell (AFD) and the single dendrite of ASC (white arrow) are contained within the sheath cell. **E:** Section approximately 9.5 μm posterior to the amphidial pore. This level shows the transition zones of twelve neurons. **F:** Section approximately 10.2 μm posterior to the amphidial pore. At this level tight junctions (TJ) form between all 13 neurons and between the neurons, the sheath cell and the shortest neuron (ASM). Scale bar in panel F=2 microns and applies to all panels.

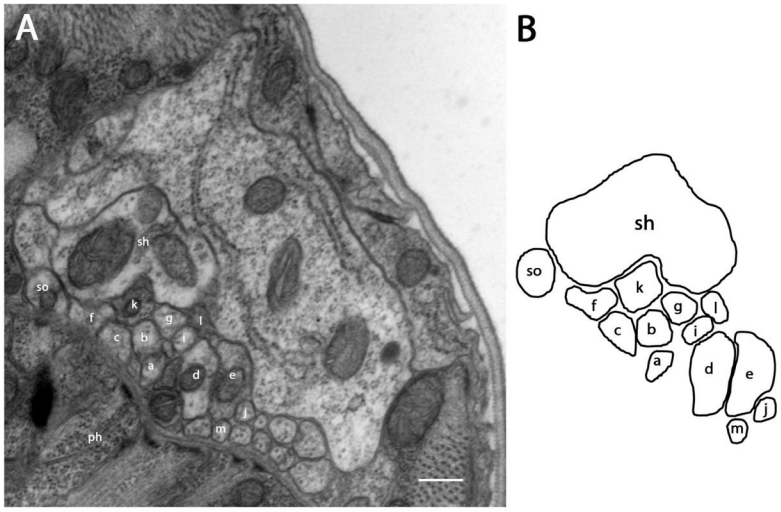

Figure 2.

Section approximately 11.2 μm posterior to the amphidial pore (1μm posterior to the tight junction region). **A:** After the tight junction region, which is at the posterior extremity of the amphidial channel, dendrites of all amphidial neurons, the socket cell and the sheath cell form a bundle and extend posteriorly to the lateral ganglion. **B:** Diagram identifies the neurons individually. Scale bar = 2 microns. Panel A corresponds to the plane labeled Fig. 2A in the three-dimensional reconstruction, Fig. 6B.

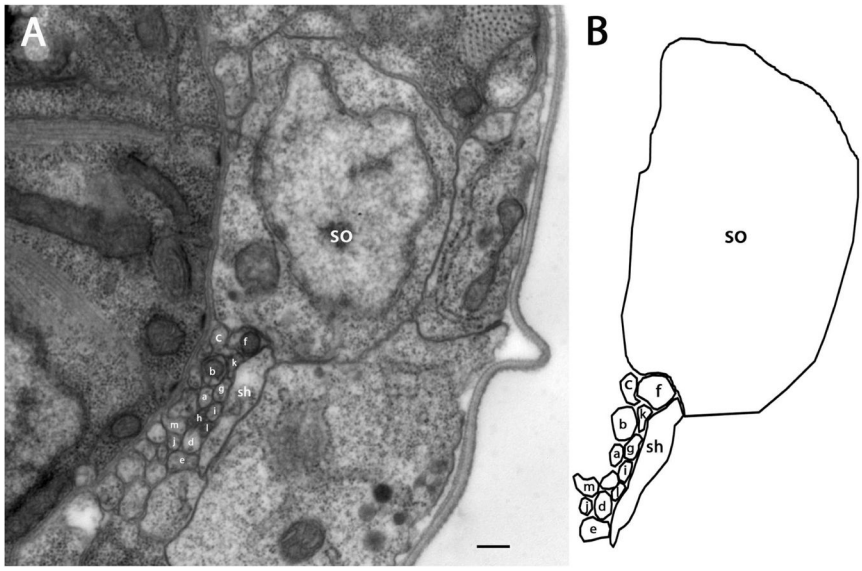

Figure 3.
Section approximately 33 μm posterior to the amphidial pore. **A:** The cell body of the socket cell is seen at this level. **B:** Diagram identifies the neurons individually Scale bar = 2 microns. Panel A corresponds to the plane labeled Fig. 3A in the three-dimensional reconstruction, Fig. 6A.

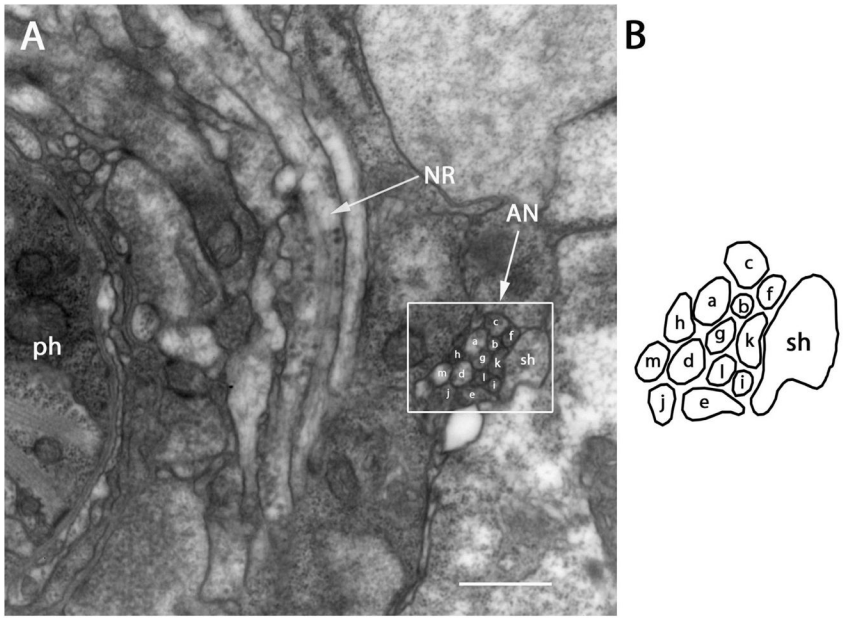

Figure 4.

Section approximately 57 μm posterior to the amphidial pore. **A:** The nerve ring (NR) is found at this level. The bundle (white box) formed by all 13 amphidial neurons (AN) and the sheath cell (sh) continues to extend posteriorly between the nerve ring and the body wall. **B:** Diagram identifies the neurons individually. Scale bar = 500 nm. Panel A corresponds to the plane labeled Fig. 4A in the three dimensional-reconstruction, Fig. 6A.

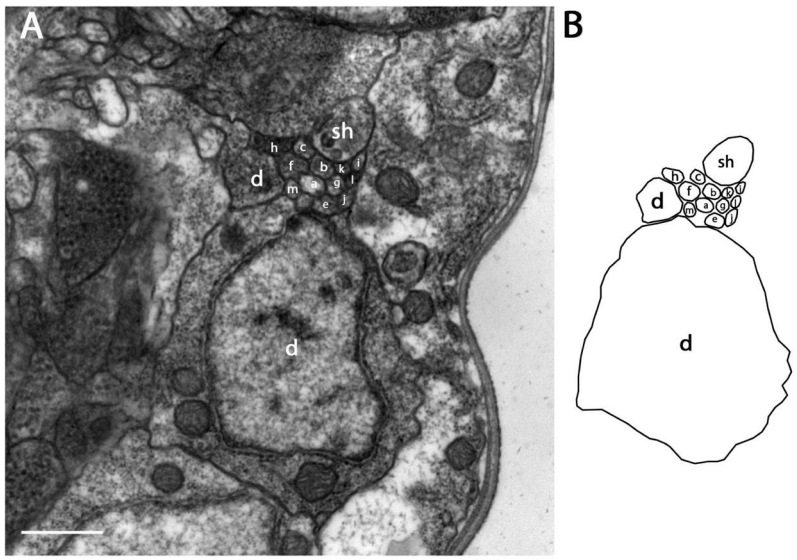

Figure 5.

Section approximately 61μm posterior to the amphidial pore. **A:** The cell body and part of the dendrite of AFD (d) are evident at this level. **B:** Diagram identifies the neurons individually. Scale bar = 500 nm. Panel A corresponds to the plane labeled Fig. 5A in the three-dimensional reconstruction, Fig. 6A.

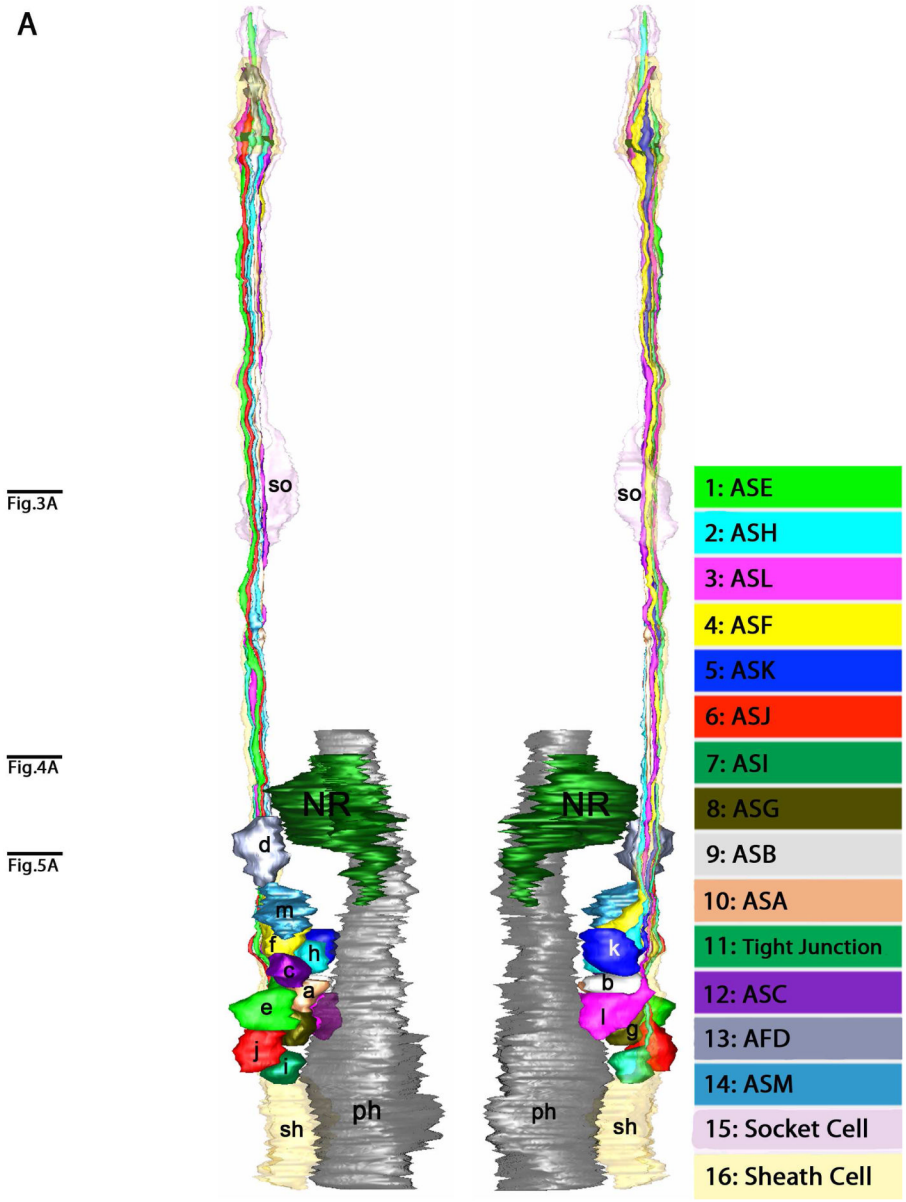

B

Fig.1A

Fig.1B

Fig.1C

Fig.1D

Fig.1E

Fig.1F

Fig.2A

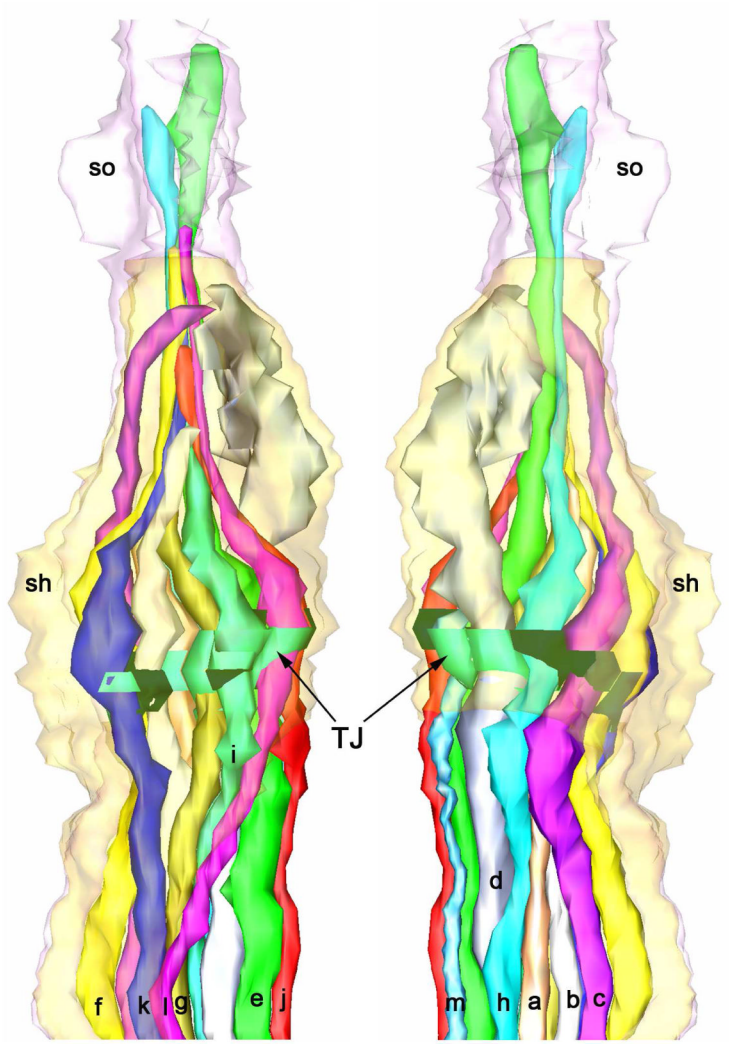

C

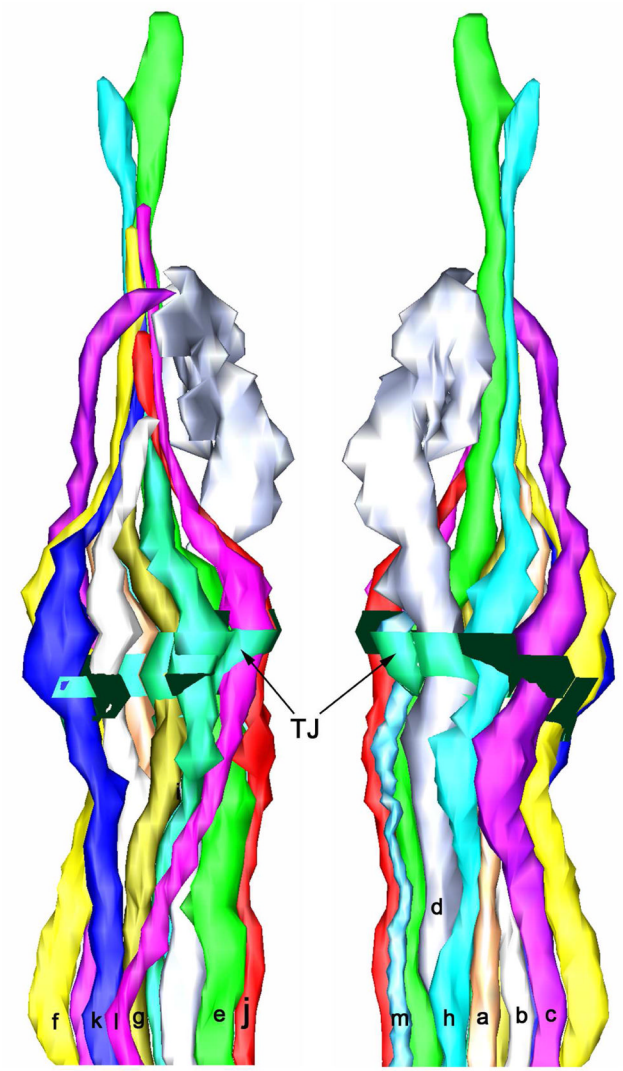

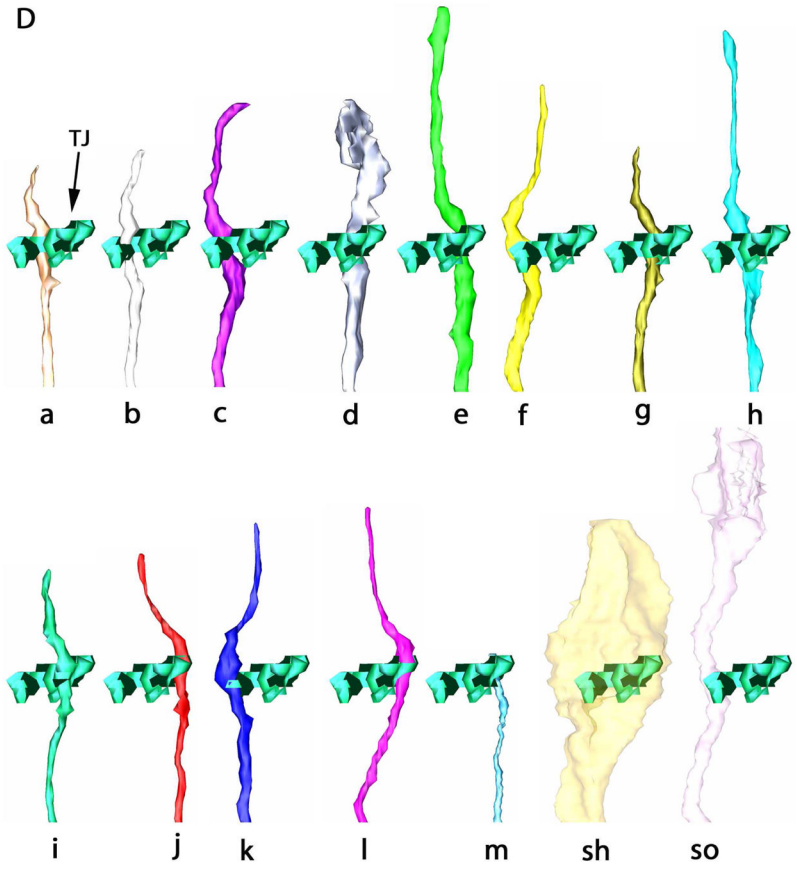

Figure 6.

Three-dimensional reconstruction of the amphidial neurons of *Parastrongyloides trichosuri*. **A:** Stereo model of a reconstruction of amphidial neurons, socket cell and sheath cell of the right amphid. Anterior is up. The dorsal aspect of the amphidial complex faces the viewer in the left image. The ventral aspect faces the viewer in the right image. Black lines with letters indicate the approximate planes of the amphid from which the images in Figs. 3A, 4A and 5A were obtained. **B.** Stereo model of the anterior extremityof the reconstruction of the right amphid. Anterior is up. The left image is viewed from the right side of the animal. The right image is viewed from the opposite side. Black lines with letters indicate the approximate planes of the amphid from which the images in Figs. 1A–F and 2A were obtained. **C:** View of reconstruction from Fig. 6B with socket cell and sheath cell removed for easier viewing of amphidial dendrites. **D.** Models of the individual amphidial dendrites, the socket cell (sd) and the sheath cell (sh). Lower case letters labeling the amphidial dendrites correspond to the third letters in the unique three-letter designations of neurons to which the dendrites belong. TJ = tight junction.

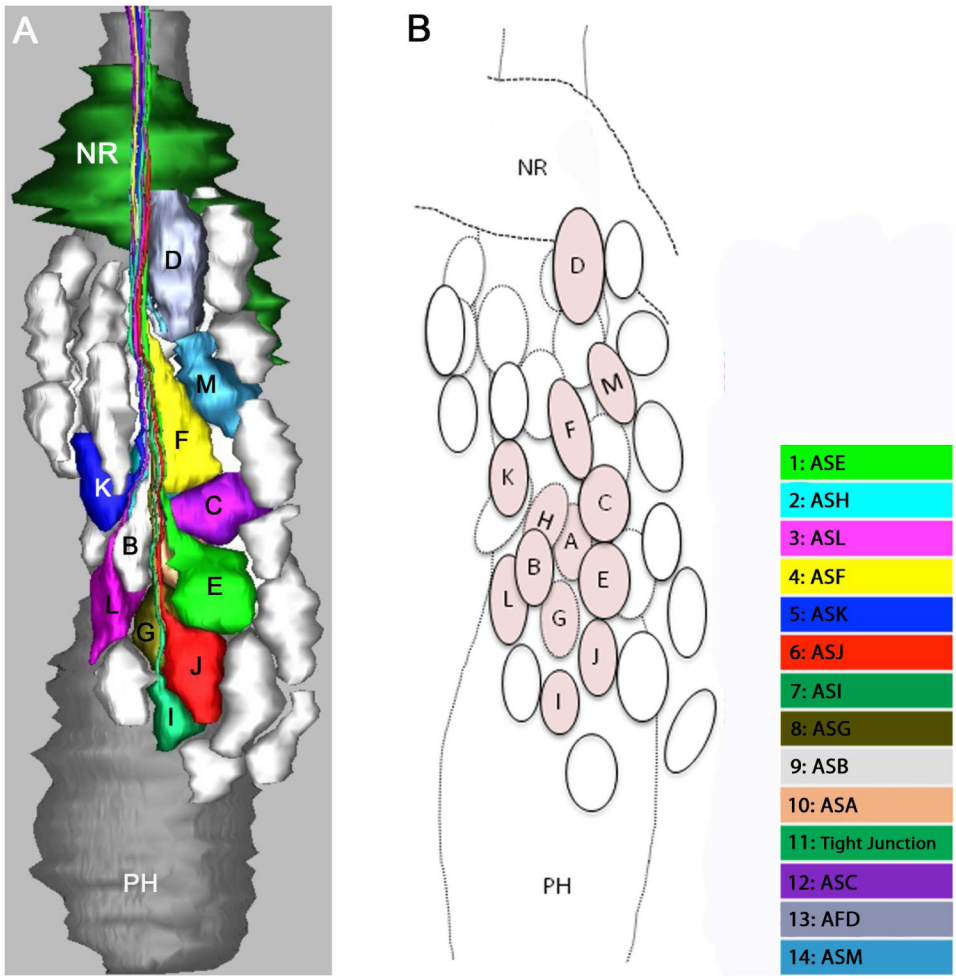

Figure 7.
Three-dimensional reconstruction of the amphidial cell bodies of *Parastrongyloides trichosuri*. Anterior is up. **A:** Model of the lateral ganglion to the right of the pharynx from a lateral view. The colored cell bodies are those of the amphidial neurons. Cell bodies of other unidentified neurons are represented in white. **B:** Diagram identifies the neuronal cell bodies individually. Amphidial cell bodies are tinted and marked with letters corresponding to the third letter of their unique three-letter designations. Unidentified cell bodies are represented as untinted ovals.

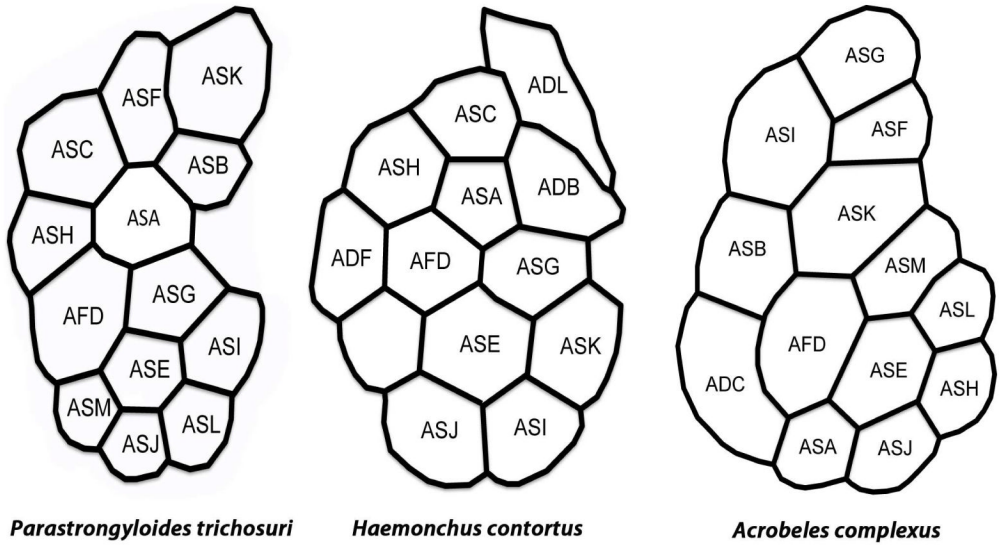

Figure 8.

Arrangement of amphidial dendrites of first-stage *Parastrongyloides trichosuri*, *Haemonchus contortus* and *Acrobeles complexus* larvae viewed in cross section at the level of the tight junction. The left side of each diagram is adjacent to the pharynx, and the top is dorsal. Three-letter designations of dendritic processes reflect adaptations of the system of nomenclature originally devised for amphidial neurons of *C. elegans* Ward et al. (1975). Data for *H. contortus* are redrawn from Li et al. (2000) and data for *A. complexus* are redrawn from Bumbarger et al. (2009).

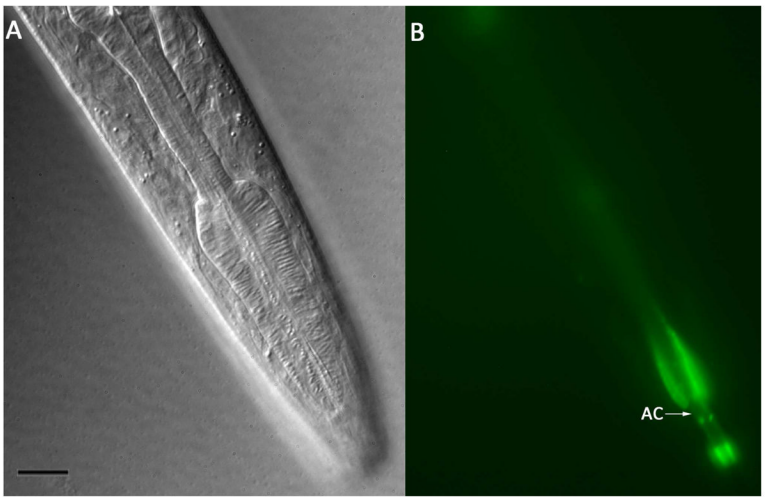

Figure 9.
Living first-stage *P. trichosuri* larva following incubation in 0.4 mg/ml FITC. **A:** DIC image showing lateral aspect of the cephalic area. Bar = 10 μm. **B:** Fluorescence image of larva in panel A showing amphidial channels (AC) filled with FITC.

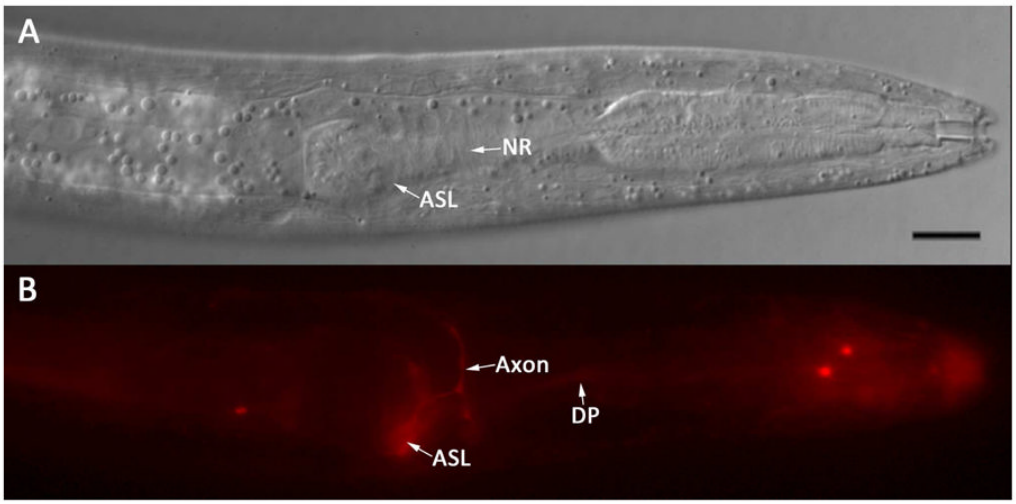

Figure 10.

Living first-stage *P. trichosuri* larva following incubation in 0.02 mg/ml DiI. **A:** DIC image showing a left lateral view of the cephalic extremity. The cell body of the amphidial neuron tentatively identified as ASL (ASL) and the nerve ring (NR) are indicated. Bar = 10 μm. **B:** Fluorescence image of the larva in A showing the cell body of ASL (ASL), its axon (Axon) and dendritic process (DP) filled with DiI.